

Representing Videos based on Scene Layouts for Recognizing Agent-in-Place Actions

Ruichi Yu^{1,2} Hongcheng Wang² Ang Li^{3*}
Jingxiao Zheng¹ Vlad I. Morariu^{4*} Larry S. Davis¹
{richyu, jxzheng, lsd}@umiacs.umd.edu
anglili@google.com morariu@adobe.com

¹University of Maryland, College Park ²Comcast Applied AI Research
³DeepMind ⁴Adobe Research

Abstract. We address the recognition of agent-in-place actions, which are associated with *agents* who perform them and *places* where they occur, in the context of outdoor home surveillance. We introduce a representation of the geometry and topology of scene layouts so that a network can generalize from the layouts observed in the training set to unseen layouts in the test set. This Layout-Induced Video Representation (LIVR) abstracts away low-level appearance variance and encodes geometric and topological relationships of places in a specific scene layout. LIVR partitions the semantic features of a video clip into different places to force the network to learn place-based feature descriptions; to predict the confidence of each action, LIVR aggregates features from the place associated with an action and its adjacent places on the scene layout. We introduce the Agent-in-Place Action dataset¹ to show that our method allows neural network models to generalize significantly better to unseen scenes.

1 Introduction

Recent advances in deep neural networks have brought significant improvements to many fundamental computer vision tasks, including video action recognition [1,2,3,4,5,6,7,8]. Current action recognition methods are able to detect, recognize or localize general actions and identify the agents (people, vehicles, *etc.*) performing them [1,2,3,5,6,7,8,9,10,11,12,13]. However, in applications such as surveillance, relevant actions often involve references to locations and directions—for example, it might be of interest to detect (*i.e.*, issue an alert) a person walking towards the front door of a house, but not to detect a person walking along the sidewalk. So, what makes an action "interesting" is how it interacts with the geometry and topology of the scene in which it is performed. However, the layout of even a restricted set of scenes—cameras mounted over the entrance doors of houses monitoring the fronts and backs of the houses—vary significantly.

We describe how to represent the geometry and topology of scene layouts so that a network can generalize from the layouts observed in the training set to unseen layouts in the test set. Examples of these contextualized actions in outdoor home surveillance

* This work was done while the author was at the University of Maryland.

¹ The dataset is pending legal review and will be released upon the acceptance of this paper.

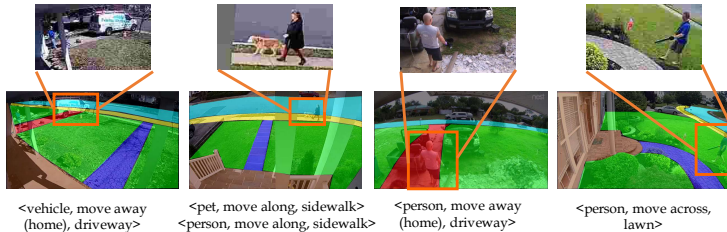


Fig. 1. Example agent-in-place actions and segmentation maps. Different colors represent different places. We zoom in to the agents performing the actions for clarity. An agent-in-place action is represented as *<agent, action, place>*.

scenarios and the semantic segmentations of scenes from which the representations are constructed as shown in Fig. 1. We will refer to these contextualized actions as "*agent-in-place*" actions to distinguish them from the widely studied generic action categories. By encoding layout information (class membership of places, layout geometry and layout topology) into the network architecture we eliminate the need to collect massive amounts of training data that would span the space of possible layouts. This allows the model to abstract away appearance variations and focus on how actions interact with the scene layouts. Without large-scale training data, a model that does not incorporate a representation of scene layout can easily overfit to the training scene layouts and exhibit poor generalization on new scenes.

To address the generalization problem, we propose *Layout-Induced Video Representation (LIVR)*, which encodes a scene layout given the segmentation map of a static scene. The representation has three components: 1) A semantic component represented by the characteristic functions of the semantic labels of the layouts (a set of bitmaps used for feature aggregation in the convolutional layers of the network referred to as "*places*"); 2) A geometric component represented by a set of coarsely quantized dis-

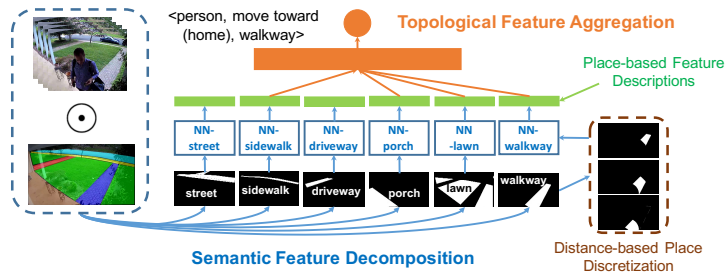


Fig. 2. Framework of LIVR. Given the segmentation map, we decompose the semantic features into different places and extract place-based feature descriptions individually, then dynamically aggregate them at inference time according to the topology of the scene. The brown part illustrates distance-based place discretization using the *walkway* semantic map as an example. \odot denotes the masking operation for spatial decomposition. "NN" stands for neural network.

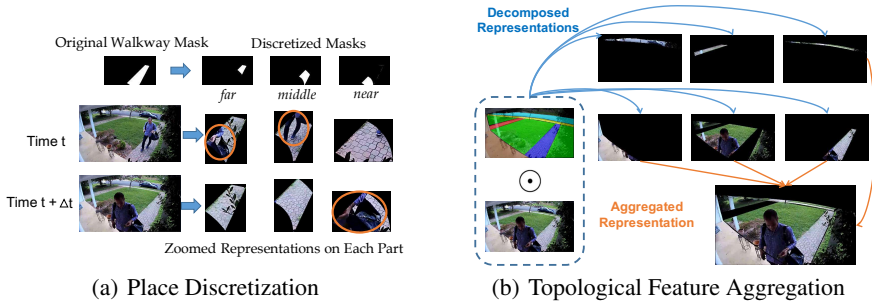


Fig. 3. (a) illustrates distance-based place discretization. We segment the bit mask representing a given semantic class based on the distance transform of a second class, to explicitly represent the spatial-temporal order of moving agents which captures the moving direction w.r.t. that place. For example, this figure shows the partition of the *walkway* map into components that are "far," "middle" and "near" to the porch class. We use *move toward (home)* action as an example: we first observe the person on the part of *far* and *middle* (distance), and after some time, the person appears in the part of *near*. We use orange ellipses to highlight person parts. (b) illustrates the motivation behind topological feature aggregation. Although the action occurs on the *walkway*, the moving person is chopped by the *walkway* mask, and part of the body appears in other places. We seek a representation that covers the entire body of the person, which can be accomplished by aggregating the masked images from places that are connected to *walkway*. To accomplish this, we use the topological connectivity between places to aggregate features.

tance transforms of each semantic place incorporated into the convolutional layers of the network; 3) A topological component represented through the connection structure in a dynamically gated fully connected layer of the network—essentially aggregating representations from adjacent (more generally h -connected for h hops in the adjacency graph of the semantic map) places. Fig. 2 shows an illustration of the proposed framework.

The first two components require *semantic feature decomposition* as shown in blue in Fig. 2. We utilize bitmaps encoded with the semantic labels of places to decompose video representations into different places and train models to learn place-based feature descriptions. This decomposition encourages the network to learn features of generic place-based motion patterns that are independent of scene layout. As part of the semantic feature decomposition, we encode scene geometry to model moving directions by discretizing a place into parts based on a quantized distance transform w.r.t. another place. Fig. 2 (brown) shows the discretized bitmaps of *walkway* w.r.t. *porch*. As illustrated in Fig. 3(a), features decomposed by those discretized bitmaps capture moving agents in spatial-temporal order, which reveals the moving direction, and can be generalized to different scene layouts. With place-based feature descriptions, we predict the confidence of an action by dynamically aggregating features within the place associated with that action and adjacent places, since the actions occurring in one place may also be projected onto adjacent places from the camera view (see Fig. 3(b)). This *topological feature aggregation* controls the "on/off" state of neuron connections from place-based

feature descriptions to action nodes at both training and testing time based on scene topological connectivity.

To evaluate LIVR, we collect a dataset called Agent-in-Place Action dataset, which consists of over 5,000 15s videos obtained from 26 different surveillance scenes with around 7,100 actions from 15 categories. To evaluate the generalization of LIVR, we split the scenes into observed and unseen scenes. Extensive experiments show that LIVR significantly improves the generalizability of the model trained on only observed scenes and tested on unseen scenes (improving the mean average precision (mAP) from around 20% to more than 51%). Consistent improvements are observed on almost all action categories.

2 Related Work

Video Understanding. Our work is related to video understanding, especially video action recognition, which takes video clips as input and categorizes the actions (usually human activities) occurring in the video. Recent work in video activity recognition explores different frameworks, *e.g.*, two-stream based models [1,2,3], RNN based models [9,10,11] and 3D ConvNets based methods [12,13,14] on different datasets [5,6,7,8]. In the context of home surveillance video understanding, prior work focuses on developing robust, efficient and accurate surveillance systems that can detect, recognize and track actions or events [15,16,17], or to detect abnormal events [18,19,20]. The most related work to ours is ReMotENet [21], which skips expensive object detection [22,23,24,25] and utilizes 3D ConvNets to detect motion of an object-of-interest in outdoor home surveillance videos. We employ a similar 3D ConvNet model as proposed in [21] as a backbone architecture for extracting place-based feature descriptions for our model. Unlike previous work, our agent-in-place actions are associated with places, and we focus on improving the generalization of a model by modeling geometrical and topological relationships in scene layouts.

Region-based Representation. Region-based representations have been widely used in computer vision tasks [26,27,28,29,30,31,32,33,34,35,36,37,38]. For example, SIFT [28] represents an image using features extracted from blobs; spatial pyramid pooling based methods partition the image into divisions and aggregate local features in them [29,30,31,32,33,34,35]; some methods utilize high-level semantic representations extracted from objects in images or actions in videos [26,36,39,40,37,38]. Li *et al.* [41] represented videos by learning from weak detection bounding boxes and pooling only features related to facial regions for video face verification. Zhao *et al.* [42] proposed an image representation based on pooling semantic features of individual objects into a feature map. Our method also leverages region-based representations, but we decompose regions based on scene layout to extract place-based features and aggregate them according to scene topology. Our method abstracts complex scene layouts to learn scene-independent features to generalize to unseen scenes.

Knowledge Transfer. The biggest challenge of agent-in-place action recognition is to generalize a model trained with limited scenes to unseen scenes. Previous work on knowledge transfer in both image and video domain has been based on visual similarity, which requires a large amount of training data [43,44,45,46,47,48,49]. For trajectory

prediction, Ballan *et al.* [43] transferred the priors of statistics from training scenes to new scenes based on scene similarity. Kitani *et al.* [50] extracted static scene features to learn scene-specific motion dynamics for predicting human activities. Instead of utilizing low-level visual similarity for knowledge transfer, our video representation abstracts away appearance and location variance and models geometrical and topological relationships in a scene.

3 Layout-Induced Video Representation

3.1 Framework Overview

The network architecture of the layout-induced video representation is shown in Fig. 4. For each video, we stack sampled frames of a video clip into a 4-D input tensor. Frame differences are used as the input since they suppress the influence of scene background and encourage the model to capture more abstract visual concepts [21]. Our backbone network is similar to the architecture of ReMotENet [21], which is composed of 3D Convolution (3D-conv) blocks. A key component of our framework is semantic feature decomposition, which decomposes feature maps according to region semantics obtained from given segmentation masks. This feature decomposition can be applied after any 3D-conv layer. Spatial Global Max Pooling (SGMP) is applied to extracted features within places, allowing the network to learn abstract features independent of shapes, sizes and absolute coordinates of both places and moving agents. For predicting each action label, we aggregate features from different places based on their connectivity in the segmentation map, referred to as Topological Feature Aggregation.

3.2 Semantic Feature Decomposition

Semantic Feature Decomposition utilizes a segmentation map of each place to decompose features and force the network to extract place-based feature descriptions individually. The segmentation maps are manually constructed using the LabelMe online annotation tool² to annotate each place by drawing points to construct polygons. In addition, to differentiate some of the actions *e.g.*, *<person, move toward (home), walkway>* and *<person, move away (home), walkway>*, we extend our place descriptions by segmenting a place into several parts based on its distance to an anchor place to allow the network to explicitly model moving directions with respect to the anchor place.

Place-based Feature Descriptions (PD). Given a segmentation map, we extract place-based feature descriptions as shown in the blue boxes in Fig. 4. We first use the segmentation map represented by a set of binary masks to decompose feature maps spatially into regions, each capturing the motion occurring in a certain place. The decomposition is applied to features instead of raw inputs to retain context information³. Let

² <http://labelme.csail.mit.edu/>

³ An agent can be located at one place, but with part of its body projected onto another place in the view of the camera. If we use the binary map as a hard mask at input level, then for some places such as *sidewalk*, *driveway* and *walkway*, only a small part of the moving agents will remain after the masking operation.

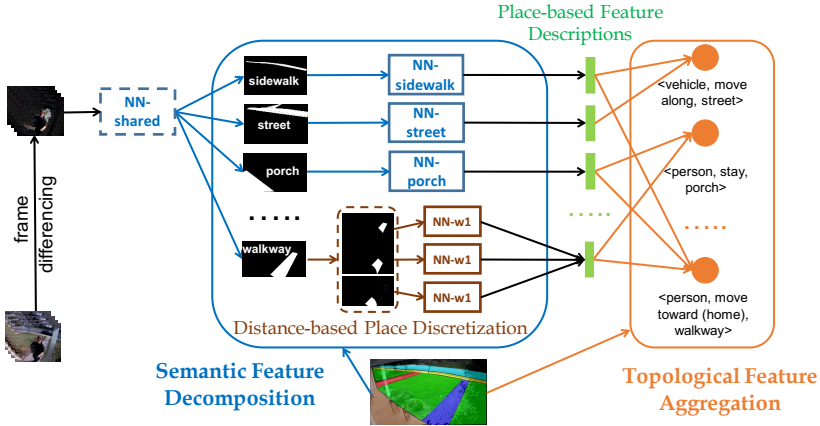


Fig. 4. Layout-induced Video Representation Network: The dashed blue box indicates a shared 3D ConvNet to extract low-level features. We utilize the segmentation maps to decompose features into different places, and the solid blue boxes indicate that we train place-based models to extract place-based feature descriptions. When relevant to the activities of interest, we conduct distance-based place discretization to model moving directions; finally, we leverage the connectivity of places to aggregate the place-based feature descriptions at inference level.

$\mathbf{X}_L \in \mathbb{R}^{w_L \times h_L \times t_L \times c}$ be the output tensor of the L^{th} conv block, where w_L, h_L, t_L denote its width, height and temporal dimensions, and c is the number of feature maps. The place-based feature description of a place indexed with p is

$$f_{L,p}(\mathbf{X}_L) = \mathbf{X}_L \odot \mathbb{I}[\mathbf{M}_L = p] \quad (1)$$

where $\mathbf{M}_L \in \mathbb{I}^{w_L \times h_L \times 1}$ is the segmentation index map and \odot is a tiled element-wise multiplication which tiles the tensors to match their dimensions. Place descriptions can be extracted from different levels of feature maps. $L = 0$ means the input level; $L > 0$ means after the L^{th} 3D-conv blocks. A higher L generally allows the 3D ConvNet to observe more context and abstract features. We treat L as a hyper-parameter of the framework and study its effect in Sec. 5.

Distance-based Place Discretization (DD). Many actions are naturally associated with moving directions *w.r.t.* some scene element (*e.g.*, the house in home surveillance). To learn general patterns of the motion direction in different scenes, we further discretize the place segmentation into several parts, and extract features from each part and aggregate them to construct the place-based feature description of this place. For illustration, we use *porch* as the anchor place (shown in Fig. 5(a)). We compute the distance between each pixel and the *porch* in a scene (distance transform), and segment a place into k parts based on their distances to *porch*. The left bottom map in 5(a) shows the porch distance transform of a scene. Let $D_L(x)$ be the distance transform of a pixel location x in the L^{th} layer. The value of a pixel x in the part indexing map \mathbf{M}_L^{Δ} is

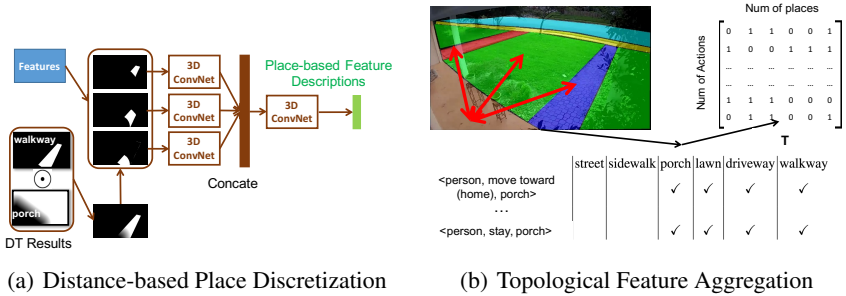


Fig. 5. (a) shows the process of distance-based place discretization. (b) shows the topological feature aggregation which utilizes the connectivities between different places in a scene to guide the connections between the extracted place-based feature descriptions and the prediction labels. For clear visualization, we use the source places as *porch* in (b) with $h = 1$. The \checkmark indicates we aggregate features from a certain place to infer the probability of an action.

computed as

$$M_L^\Delta(x) = \left\lfloor \frac{D_L^{\max}(x) - D_L^{\min}(x)}{k(D_L(x) - D_L^{\min}(x))} \right\rfloor \quad (2)$$

where $D_L^{\max}(x) = \max\{D_L(x') | M_L(x') = M_L(x)\}$ and $D_L^{\min}(x) = \min\{D_L(x') | M_L(x') = M_L(x)\}$ are the max and min of pixel distances in the same place. They can be efficiently pre-computed. The feature description corresponding to the i^{th} part of p^{th} place in L^{th} layer is

$$f_{L,p,i}^\Delta(\mathbf{X}_L) = \mathbf{X}_L \odot \mathbb{I}[\mathbf{M}_L = p \wedge \mathbf{M}_L^\Delta = i] \quad (3)$$

where \odot is the tiled element-wise multiplication.

Discretizing a place into parts at different distances to the anchor place and explicitly separating their spatial-temporal features allows the representation to capture moving agents in spatial-temporal order and extract direction-related abstract features. However, not all places need to be segmented since some places (such as *sidewalk*, *street*) are not associated with any direction-related action (e.g., moving toward or away from the house). For these places, we still extract the whole-place feature descriptors $f_{L,p}$. We will study the different choices of place discretization and the number of parts k in Sec. 5. To preserve temporal ordering, we apply 3D-conv blocks with spatial-only max pooling to extract features from each discretized place, and concatenate them channel-wise. Then, we apply 3D-conv blocks with temporal-only max pooling to abstract temporal information. Finally, we obtain a 1-D place-based feature description after applying GMP (see Fig.5(a)). It is worth noting that the final description obtained after distance-based place discretization has the same dimensions as non-discretized place descriptions.

3.3 Topological Feature Aggregation (Topo-Agg)

Semantic feature decomposition allows us to extract a feature description for each place individually. In order to predict action labels, these place features need to be aggregated. Each action is one-one mapped to a place. To predict the confidence of an action a occurring in a place p , features extracted far from place p are distractors. To reduce interference by features from irrelevant places, we structure the network to ignore these far away features using *Topological Feature Aggregation*, which utilizes the spatial connectivity between places, to guide feature aggregation.

Specifically, as shown in Fig. 5(b), given a scene segmentation map, a source place p and a constant h , we employ a Connected Component algorithm to find the h -connected set $C_h(p)$ which contains all places connected to place p within h hops. The constant h specifies the minimum number of steps to walk from the source to a destination place. Given the h -connected place set C_h , we construct a binary action-place matrix ($\mathbf{T} \in \mathbb{R}^{n_a \times n_p}$) for the scene where n_a is the number of possible actions and n_p is the number of places. $\mathbf{T}_{i,j} = 1$ if and only if place j is in the C_h of the place corresponding to action i . Fig. 5(b) shows an example segmentation map with its action-place mapping, where $C_0(\text{porch}) = \{\text{porch}\}$, $C_1(\text{porch}) = \{\text{porch}, \text{walkway}, \text{driveway}, \text{lawn}\}$, $C_2(\text{porch})$ includes all except for *street*, and $C_3(\text{porch})$ covers all six places.

We implement topological feature aggregation at both training and testing using a gated fully connected layer with customized connections determined by the action-place mapping \mathbf{T} . Given n_p m -D features extracted from n_p places, we concatenate them to form a $(n_p \times m)$ -D feature vector. We use \mathbf{T} to determine the "on/off" status of each connection of a layer between the input features and the output action confidences. Let $\mathbf{T}_* = \mathbf{T} \otimes \mathbb{I}^{1 \times m}$ be the actual mask applied to the weight matrix $\mathbf{W} \in \mathbb{R}^{n_a \times n_p m}$ where \otimes is the matrix Kronecker product. The final output is computed by

$$\mathbf{y} = (\mathbf{W} \odot \mathbf{T}_*) \mathbf{f}_* \quad (4)$$

where \odot is element-wise matrix multiplication, \mathbf{f}_* is the concatenated feature vector as the input of the layer. We omit bias for simplicity. Let J be the training loss function (cross-entropy loss), considering the derivative of \mathbf{W} , the gradient formulation is

$$\nabla_{\mathbf{W}} J = (\nabla_{\mathbf{y}} J \mathbf{f}_*^T) \odot \mathbf{T}_* \quad (5)$$

which is exactly the usual gradient $(\nabla_{\mathbf{y}} J \mathbf{f}_*^T)$ masked by \mathbf{T}_* . At training time, we only back-propagate the gradients to connected neurons. We also experiment with multiple fully connected layers, discussed in Sec. 5.

4 Agent-in-Place Action Dataset

We introduce a surveillance video dataset for recognizing agent-in-place actions. We collected outdoor home surveillance videos from internal donors and webcams⁴ for months to obtain over 7, 100 actions from around 5, 000 15-second video clips with

⁴ <http://www.nestcamdirectory.com/>

1280 × 720 resolution. These videos are captured from 26 different outdoor cameras which cover various layouts of typical American families’ front yards and back yards.

We select 15 common agent-in-place actions to label and each is represented as a tuple containing an action, the agent performing it, and the place where it occurs. The agents, actions, and places involved in our dataset are: $Agent = \{person, vehicle, pet\}$; $Action = \{move\ along, stay, move\ away\ (home), move\ toward\ (home), interact\ with\ vehicle, move\ across\}$; $Place = \{street, sidewalk, lawn, porch, walkway, driveway\}$.

The duration of each video clip is 15s, so multiple actions can be observed from a single agent or multiple agents in one video. We formulate action recognition as a multi-label classification task. We split the 26 cameras into two sets: observed scenes (5) and unseen scenes (21) to balance the number of instances of each action in observed and unseen scenes and at the same time cover more scenes in the unseen set. We train and validate our model on observed scenes, and test its generalization capability on the unseen scenes. The detailed statistics of our cleaned dataset is shown in Fig. 6.

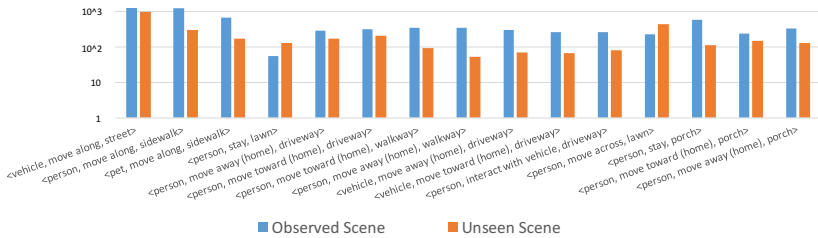


Fig. 6. Dataset Statistics on observed and unseen scenes.

5 Experiments

5.1 Implementation Details

Network Architecture. Unlike traditional 3D ConvNets which conduct spatial-temporal max-pooling simultaneously, we found that decoupling the pooling into spatial-only and temporal-only leads to better performance (experimental results and discussions can be found in the supplementary materials). So, for each place-specific network that extracts place-based feature descriptions, we utilize nine blocks of 3D ConvNets with the first five blocks using spatial-only max pooling and the last four blocks using temporal-only max pooling. The first two blocks have one 3D-conv layer each, and there are two convolutional (conv) layers with ReLU in between for the remaining blocks. For each place-specific network, we use $64 \times 3 \times 3 \times 3$ conv filters per 3D-conv layer. After conducting SGMP on features extracted by each place-specific network, the final concatenated 1-D feature dimension is 6×64 since there are 6 places in total. The inference is conducted with a gated fully connected layer, whose connections ("on/off" status) are determined by action labels and scene topology. We use the sigmoid function to obtain

the predicted probability of each action. It is worth noting that if we conduct feature level decomposition ($L > 0$), we use a shared network to extract low-level features. The detailed place-specific network structure is shown in Table 1.

Anchor Place. For our dataset, the directions mentioned are all relative to the house location, and *porch* is a strong indicator of the house location. So we only conduct distance transform to *porch*⁵, but the distance-based place discretization method can be easily generalized to represent moving direction w.r.t any arbitrary anchor place.

Training and Testing Details. Our action recognition task is formulated as multi-label classification without mutual exclusion. The network is trained using the Adam optimizer [51] with 0.001 initial learning rate. For input video frames, we follow [21] to use FPS 1 and down-sample each frame to 160×90 to construct a $15 \times 160 \times 90 \times 3$ tensor for each video as input. Suggested by [21], small FPS and low resolution are sufficient to model actions for home surveillance where most agents are large and the motion patterns of actions are relatively simple. We evaluate the performance of recognizing each action independently and report Average Precision (AP) for each action and mean Average Precision (mAP) over all categories.

Hyperparameter Selection. We split the 26 scenes into two sets: observed scenes and unseen scenes. We further split the videos in observed scenes into training and validation sets with a sample ratio of nearly 1 : 1. We train our model on observed scenes and test it on unseen scenes. The validation set is used for tuning hyperparameters: we decompose semantics after the second conv blocks ($L = 2$); we conduct distance-based place discretization on $PLDT = \{\textit{walkway}, \textit{driveway}, \textit{lawn}\}$ and choose $k = 3$; for topological feature aggregation, we choose $h = 1$.

Table 1. Network Structure of LIVR. We apply spatial-only max pooling after block Conv1-Conv5, and temporal-only max pooling after block Conv6-Conv9. From Conv3 to Conv9, each conv blocks consists of two identical 3D-conv layers with ReLU in between. The "on/off" status of each connection for the final gated FC layer is determined by Topo-Agg.

Block	Input Size	Kernel Size	Stride	# Filters	Block	Input Size	Kernel Size	Stride	# Filters
Conv1	$15 \times 90 \times 160 \times 3$	$3 \times 3 \times 3$	$1 \times 1 \times 1$	64	Conv6	$15 \times 3 \times 5 \times 64$	$3 \times 3 \times 3$	$1 \times 1 \times 1$	64
Pool1	$15 \times 90 \times 160 \times 3$	$1 \times 2 \times 2$	$1 \times 2 \times 2$	-	Pool6	$15 \times 3 \times 5 \times 64$	$2 \times 1 \times 1$	$2 \times 1 \times 1$	-
Conv2	$15 \times 45 \times 80 \times 64$	$3 \times 3 \times 3$	$1 \times 1 \times 1$	64	Conv7	$8 \times 3 \times 5 \times 64$	$3 \times 3 \times 3$	$1 \times 1 \times 1$	64
Pool2	$15 \times 45 \times 80 \times 64$	$1 \times 2 \times 2$	$1 \times 2 \times 2$	-	Pool7	$8 \times 3 \times 5 \times 64$	$2 \times 1 \times 1$	$2 \times 1 \times 1$	-
Conv3	$15 \times 23 \times 40 \times 64$	$3 \times 3 \times 3$	$1 \times 1 \times 1$	64	Conv8	$4 \times 3 \times 5 \times 64$	$3 \times 3 \times 3$	$1 \times 1 \times 1$	64
Pool3	$15 \times 23 \times 40 \times 64$	$1 \times 2 \times 2$	$1 \times 2 \times 2$	-	Pool8	$4 \times 3 \times 5 \times 64$	$2 \times 1 \times 1$	$2 \times 1 \times 1$	-
Conv4	$15 \times 12 \times 20 \times 64$	$3 \times 3 \times 3$	$1 \times 1 \times 1$	64	Conv9	$2 \times 3 \times 5 \times 64$	$3 \times 3 \times 3$	$1 \times 1 \times 1$	64
Pool4	$15 \times 12 \times 20 \times 64$	$1 \times 2 \times 2$	$1 \times 2 \times 2$	-	Pool9	$2 \times 3 \times 5 \times 64$	$2 \times 1 \times 1$	$2 \times 1 \times 1$	-
Conv5	$15 \times 6 \times 10 \times 64$	$3 \times 3 \times 3$	$1 \times 1 \times 1$	64	SGMP	$1 \times 3 \times 5 \times 64$	$1 \times 3 \times 5$	$1 \times 1 \times 1$	-
Pool5	$15 \times 6 \times 10 \times 64$	$1 \times 2 \times 2$	$1 \times 2 \times 2$	-	Gated FC	$1 \times 1 \times 1 \times 384$	-	-	-

5.2 Baseline Models

We follow [21] to employ 3D ConvNets as our baseline (B/L) model. All three baseline models share the same 3D ConvNets architecture, which is very similar to the architectures of each place-specific network that extracts place-based feature descriptions,

⁵ If there is no *porch* in a scene, we let the user to draw a line (click to generate two endpoints) to indicate its location

except that the last layer is fully connected instead of gated through topological feature aggregation. The difference among baseline 1, 2 and 3 is their input: B/L1 takes the raw frames as input; B/L2 applies frame difference on two consecutive frames; B/L3 incorporates the scene layout information by directly concatenating the 6 segmentation maps to the RGB channels in each frame (we call this method ConcatMap), resulting in an input of 9 channels per frame in total. We train the baseline models using the same setting as in the proposed model, and the performance of the baselines are shown in column 2-5 in Table 2. We observe that: 1) adding frame differencing leads to significant performance improvements; 2) marginal improvements are obtained by incorporating scene layout information using ConcatMap; 3) the testing performance gap between observed and unseen scenes is large, which reveals the poor generalization of the baseline models. In addition, we also train a B/L3 model with $6\times$ more filters per layer to evaluate whether model size is the key factor for the performance improvement. The result of this enlarged B/L3 model is shown in column 5 of Table 2. Overall, the baseline models which directly extract features jointly from the entire video suffer from overfitting, and simply enlarging the model size or directly using the segmentation maps as features does not improve their generalization. More details about baseline models can be found in the supplementary materials.

Table 2. The path from traditional 3D ConvNets to our methods. B/L1-B/L3 are baseline models with raw pixels, frame differencing and ConcatMap as input, respectively. For our proposed models: V1 uses segmentation maps to extract place-based feature descriptions only. V3 applies distance-based place discretization for some places. Both V1 and V3 use a FC layer to aggregate place features; V2 and V4 uses topological feature aggregation. H and FPS2 indicates using higher resolutions and FPS, and MF means using more filters per conv layer.

Network Architecture	B/L1	B/L2	B/L3	B/L3 +MF	Ours- V1	Ours- V2	Ours- V3	Ours- V4	Ours- V4+H	Ours- V4+MF	Ours- V4+FPS2
3D ConvNet?	✓	✓	✓	✓	✓	✓	✓	✓	✓	✓	✓
frame differencing?		✓	✓	✓	✓	✓	✓	✓	✓	✓	✓
ConcatMap?			✓	✓							
place-based feature description?					✓	✓	✓	✓	✓	✓	✓
distance-based place discretization?							✓	✓	✓	✓	✓
topological feature aggregation?						✓		✓	✓	✓	✓
higher resolutions?									✓		
more filters?				✓						✓	
higher FPS?											✓
Observed scenes mAP	43.34	51.79	53.54	52.02	60.17	60.97	57.64	56.71	56.26	56.01	58.93
Unseen scenes mAP	14.62	18.46	20.96	16.12	41.54	44.73	46.57	51.41	49.13	51.87	50.31

5.3 Evaluation on the Proposed Method

The path from traditional 3D ConvNets to our method. We show the path from the baselines to our method in Table 2. In column 6-9, we report the mAP of our models on observed scene validation set and unseen scene testing set. We observe three significant performance gaps, especially on unseen scenes: 1) from B/L3 to Ours-V1, we obtain over 20% mAP improvement by applying the proposed semantic feature decomposition

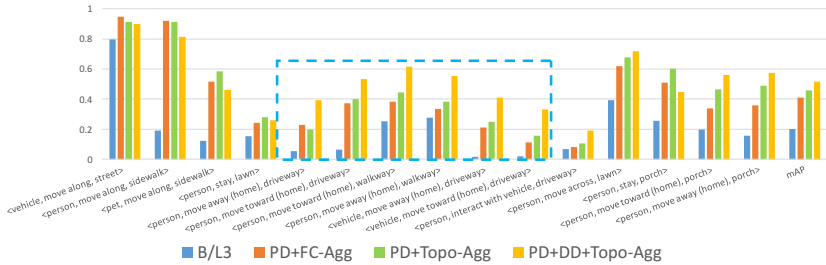


Fig. 7. Per-category average precision of the baseline 3 and our methods on unseen scenes. The blue dashed box highlights actions which require modeling moving directions. We observe that the proposed place-based feature descriptions (PD), distance-based place discretization (DD) and topological feature aggregation (Topo-Agg) significantly improve the average precision on almost all action categories. FC-Agg stands for using a FC layer to aggregate place descriptions.

to extract place feature descriptions; 2) from Ours-V1 to Ours-V3, our model is further improved by explicitly modeling moving directions by place discretization; 3) when compared to using a fully connected layer for feature aggregation (V1 and V3), our topological method (V2 and V4) leads to another significant improvement, which shows the efficacy of feature aggregation based on scene layout connectivity. We also evaluate the effect of resolutions, FPS and number of filters using our best model (Ours-V4). Doubling the resolution (320×180), FPS (2) and number of filters (128) only results in a slight change of the model’s accuracy (columns 10-12 in Table 2).

Per-category Performance. Fig. 7 shows the average precision for each action on unseen scenes. Our method outperforms the baseline methods by a large margin on almost all action categories. When comparing the orange and green bars in Fig. 7, we observe that the proposed topological feature aggregation (Topo-Agg) leads to consistently better generalization for almost all actions. The blue dashed box highlights the actions that include moving directions, and consistent improvements are brought by distance-based place discretization (DD). For some actions, especially the ones occurring on street and sidewalk, since they are relatively easy to recognize, adding DD or Topo-Agg upon the place-based feature descriptions (PD) does not help much. Overall, our layout-induced video representation improves the generalization capability of the network, especially for actions that are more challenging, and are associated with moving directions.

Qualitative Results. Some example actions are visualized using three frames in temporal order and the predicted probabilities of the groundtruth actions using different methods are reported in Fig. 8. It is observed that for relatively easy actions such as <vehicle, move along, street>, performance is similar across approaches. However, for challenging actions, especially ones requiring modeling moving directions such as <person, move toward (home), walkway>, our method outperforms baselines significantly.



Fig. 8. Qualitative examples: The predicted confidences of groundtruth actions using different methods. We use 3 frames to visualize a motion and orange ellipses to highlight moving agents.

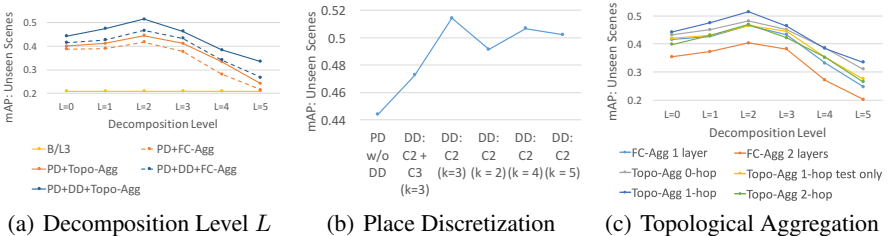


Fig. 9. Evaluation: (a) The effect of extracting place-based feature descriptions (PD) at different levels using different variants of our proposed model. The best performance is achieved when PD is conducted at feature level after the second 3D-conv blocks. (b) Different strategies for distance-based place discretization. Choosing $k = 3$ and conducting DD on *lawn*, *walkway* and *driveway* leads to the highest mAP. (c) Different feature aggregation approaches on unseen scenes. When aggregating features from places directly connected to the place where the action occurs and applying Topo-Agg at both training and testing, our model achieves its highest accuracy.

5.4 Ablation Analysis on Unseen Scenes

Place-based Feature Description. The hyper-parameter for PD is the level L , controlling when to decompose semantics in different places. Fig. 9(a) and 9(c) show that the generalization capability of our model is improved when we allow the network observe the entire video at input level, and decompose semantics at feature level (after the 2nd conv blocks). However, if we extract place descriptions after a very late block (e.g., level 4 or 5), it fails to improve the model generalizability.

Distance-based Place Discretization. We study different strategies for determining PL_{DT} and the number of parts to discretize (k) per place. From our observations,

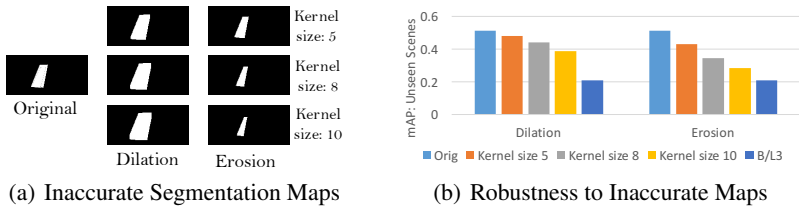


Fig. 10. (a) We use dilation and erosion to simulate two possible sources of inaccurate segmentation maps when annotated by customers. We use the map of a *walkway* as an example to show the effect of inaccurate maps to different degrees (with different kernel sizes). Larger kernel size leads to higher degree of inaccuracy. (b) The performance of our full model trained with different degrees of inaccurate segmentation maps. Our method is more robust to dilation than erosion.

including the anchor *place-porch*, the six places in our dataset can be clustered into three categories with regard to the distance to camera: C1 includes only *porch*, which is usually the closest place to camera; C2 includes *lawn*, *walkway*, *driveway*, and actions occurring in those places usually require modeling the moving direction directly; C3 includes *sidewalk* and *street*, which are usually far away from the house, and actions on them are not sensitive to directions (e.g., “*move along*”). We evaluate our method with two strategies to apply DD on: 1) all places belong to C2 and C3; 2) only places in C2. The results are shown in Fig. 9(b). We observe that applying DD on C3 does not help much, but if we only apply DD on places in C2, our method achieves the best performance. In terms of the number of discretized parts k , we evaluate k from 2 to 5 and observe from Fig. 9(b) that the performance is robust when $k \geq 3$.

Topological Feature Aggregation. We evaluate different h values to determine the h -connected set and different strategies to construct and utilize the action-place mapping \mathbf{T} . The results are shown in Fig. 9(c). We observe that Topo-Agg achieves its best performance when $h = 1$, *i.e.*, for an action occurring in place P , we aggregate features extracted from place P and its directly connected places. In addition, we compare Topo-Agg to the naive fully connected inference layer (FC-Agg: 1 layer) and two fully-connected layers with 384 neurons each and a ReLU layer in between (FC-Agg: 2 layers). Unsurprisingly, we observe that the generalizability drops significantly with an extra fully-connected layer, which reflects overfitting. Our Topo-Agg outperforms both methods. We also conduct an experiment where we train a fully connected inference layer and only aggregate features based on topology at testing time (“Topo-Agg: 1-hop test only”) and it shows worse performance.

Sensitivity to Segmentation Maps. While future work includes integrating semantic segmentation into the network architecture, the model described here uses a given semantic map created by people. To explore the sensitivity of the network to typical errors that would be encountered with automatically constructed semantic maps, we apply dilation and erosion on the groundtruth maps to simulate the two situations which model inaccuracy. An example of inaccurate maps due to dilation and erosion with different kernel sizes is shown in Fig. 10(a), and the results of our method using PD+DD+Topo-

Agg with the manipulated maps are shown in Fig. 10(b). There is some performance degradation, but our method still shows significant improvements over the baselines. In addition, our method is more robust to dilation than erosion, since with large erosion kernels, the network can barely observe the motion patterns in a place.

6 Conclusions and Future Directions

To improve the generalization of a deep network that learns from limited training scenes, we propose a layout-induced video representation which abstracts away low-level appearance variance but encodes the semantics, geometry and topology of scene layout. There are two possible directions of interesting future work: first, in this paper we construct the segmentation maps manually, but we may integrate the estimation of the semantic maps into the network architecture, which may require collecting more scenes for training. Second, we may extend the task from action classification with a closed action set to a more flexible compositional and structural prediction of arbitrary agents, places and actions and associate them to form agent-in-place actions, including zero-shot actions consisting of observed agents, places and actions.

References

1. Feichtenhofer, C., Pinz, A., Zisserman, A.: Convolutional two-stream network fusion for video action recognition. In: 2016 IEEE Conference on Computer Vision and Pattern Recognition, CVPR 2016, Las Vegas, NV, USA, June 27-30, 2016. (2016) 1933–1941
2. Simonyan, K., Zisserman, A.: Two-stream convolutional networks for action recognition in videos. In: Proceedings of the 27th International Conference on Neural Information Processing Systems - Volume 1. NIPS'14, Cambridge, MA, USA, MIT Press (2014) 568–576
3. Wang, L., Xiong, Y., Wang, Z., Qiao, Y., Lin, D., Tang, X., Val Gool, L.: Temporal segment networks: Towards good practices for deep action recognition. In: ECCV. (2016)
4. Xu, C., Corso, J.J.: Actor-action semantic segmentation with grouping-process models. In: Proceedings of IEEE Conference on Computer Vision and Pattern Recognition. (2016)
5. Kuhne, H., Jhuang, H., Garrote, E., Poggio, T., Serre, T.: Hmdb: A large video database for human motion recognition. In: IEEE International Conference on Computer Vision (ICCV). (2011)
6. Soomro, K., Zamir, A.R., Shah, M.: Ucf101: A dataset of 101 human actions classes from videos in the wild. CoRR [abs/1212.0402](#) (2012)
7. Kay, W., Carreira, J., Simonyan, K., Zhang, B., Hillier, C., Vijayanarasimhan, S., Viola, F., Green, T., Back, T., Natsev, P., Suleyman, M., Zisserman, A.: The kinetics human action video dataset. CoRR [abs/1705.06950](#) (2017)
8. Caba Heilbron, F., Escorcia, V., Ghanem, B., Carlos Niebles, J.: Activitynet: A large-scale video benchmark for human activity understanding. In: The IEEE Conference on Computer Vision and Pattern Recognition (CVPR). (June 2015)
9. Donahue, J., Hendricks, L.A., Guadarrama, S., Rohrbach, M., Venugopalan, S., Darrell, T., Saenko, K.: Long-term recurrent convolutional networks for visual recognition and description. In: CVPR, IEEE Computer Society (2015) 2625–2634
10. Ng, J.Y.H., Hausknecht, M.J., Vijayanarasimhan, S., Vinyals, O., Monga, R., Toderici, G.: Beyond short snippets: Deep networks for video classification. In: CVPR, IEEE Computer Society (2015) 4694–4702

11. Ma, C., Chen, M., Kira, Z., AlRegib, G.: TS-LSTM and temporal-inception: Exploiting spatiotemporal dynamics for activity recognition. *CoRR* **abs/1703.10667** (2017)
12. Tran, D., Bourdev, L.D., Fergus, R., Torresani, L., Paluri, M.: Learning spatiotemporal features with 3d convolutional networks. In: *IEEE International Conference on Computer Vision (ICCV)*. (2015)
13. Taylor, G.W., Fergus, R., LeCun, Y., Bregler, C.: Convolutional learning of spatio-temporal features. In: *Proceedings of the 11th European Conference on Computer Vision: Part VI. ECCV'10, Berlin, Heidelberg, Springer-Verlag* (2010) 140–153
14. Ji, S., Xu, W., Yang, M., Yu, K.: 3d convolutional neural networks for human action recognition. *IEEE Trans. Pattern Anal. Mach. Intell.* **35**(1) (January 2013) 221–231
15. Haritaoglu, I., Harwood, D., Davis, L.S.: W4: Real-time surveillance of people and their activities. *IEEE Transactions on Pattern Analysis and Machine Intelligence* **22** (2000) 809–830
16. Fusier, F., Valentin, V., Brémont, F., Thonnat, M., Borg, M., Thirde, D., Ferryman, J.: Video understanding for complex activity recognition. *Machine Vision and Applications* **18**(3) (Aug 2007) 167–188
17. Collins, R., Lipton, A., Kanade, T., Fujiyoshi, H., Duggins, D., Tsin, Y., Tolliver, D., Enomoto, N., Hasegawa, O.: A system for video surveillance and monitoring. Technical Report CMU-RI-TR-00-12, Carnegie Mellon University, Pittsburgh, PA (May 2000)
18. Zhou, S., Shen, W., Zeng, D., Fang, M., Wei, Y., Zhang, Z.: Spatial-temporal convolutional neural networks for anomaly detection and localization in crowded scenes. *Image Commun.* **47**(C) (September 2016) 358–368
19. Hasan, M., Choi, J., Neumann, J., Roy-Chowdhury, A.K., Davis, L.S.: Learning temporal regularity in video sequences. In: *The IEEE Conference on Computer Vision and Pattern Recognition (CVPR)*. (June 2016)
20. Xu, D., Ricci, E., Yan, Y., Song, J., Sebe, N.: Learning deep representations of appearance and motion for anomalous event detection. In Xianghua Xie, M.W.J., Tam, G.K.L., eds.: *Proceedings of the British Machine Vision Conference (BMVC)*, BMVA Press (September 2015) 8.1–8.12
21. Yu, R., Wang, H., Davis, L.: Remotenet: Efficient relevant motion event detection for large-scale home surveillance videos. In: *IEEE Winter Conf. on Applications of Computer Vision (WACV)*. (2018)
22. Ren, S., He, K., Girshick, R., Sun, J.: Faster r-cnn: Towards real-time object detection with region proposal networks. In Cortes, C., Lawrence, N.D., Lee, D.D., Sugiyama, M., Garnett, R., eds.: *Advances in Neural Information Processing Systems* 28. Curran Associates, Inc. (2015) 91–99
23. Girshick, R.: Fast R-CNN. In: *Proceedings of the International Conference on Computer Vision (ICCV)*. (2015)
24. Gao, M., Li, A., Yu, R., Morariu, V.I., Davis, L.S.: C-wsl: Count-guided weakly supervised localization. *arXiv preprint arXiv:1711.05282* (2017)
25. Gao, M., Yu, R., Li, A., Morariu, V.I., Davis, L.S.: Dynamic zoom-in network for fast object detection in large images. *IEEE Conference on Computer Vision and Pattern Recognition (CVPR)* (2018)
26. Li, L.J., Su, H., Lim, Y., Fei-Fei, L.: Object bank: An object-level image representation for high-level visual recognition. *Int. J. Comput. Vision* **107**(1) (March 2014) 20–39
27. Sivic, J., Zisserman, A.: Video Google: A text retrieval approach to object matching in videos. In: *Proceedings of the International Conference on Computer Vision. Volume 2*. (October 2003) 1470–1477
28. Lowe, D.G.: Distinctive image features from scale-invariant keypoints. *International Journal of Computer Vision* **60** (2004) 91–110

29. Grauman, K., Darrell, T.: The pyramid match kernel: Discriminative classification with sets of image features. In: IN ICCV. (2005) 1458–1465
30. Lazebnik, S., Schmid, C., Ponce, J.: Beyond bags of features: Spatial pyramid matching for recognizing natural scene categories. In: Proceedings of the 2006 IEEE Computer Society Conference on Computer Vision and Pattern Recognition - Volume 2. CVPR '06, Washington, DC, USA, IEEE Computer Society (2006) 2169–2178
31. Yang, J., Yu, K., Gong, Y., Huang, T.: Linear spatial pyramid matching using sparse coding for image classification. In: in IEEE Conference on Computer Vision and Pattern Recognition (CVPR). (2009)
32. Wang, J., Yang, J., Yu, K., Lv, F., Huang, T., Gong, Y.: Locality-constrained linear coding for image classification. In: IN: IEEE CONFERENCE ON COMPUTER VISION AND PATTERN CLASSIFICATION. (2010)
33. Perronnin, F., Sánchez, J., Mensink, T.: Improving the fisher kernel for large-scale image classification. In: Proceedings of the 11th European Conference on Computer Vision: Part IV. ECCV'10, Berlin, Heidelberg, Springer-Verlag (2010) 143–156
34. van de Sande, K.E.A., Uijlings, J., Gevers, T., Smeulders, A.: Segmentation as Selective Search for Object Recognition. In: ICCV. (2011)
35. He, K., Zhang, X., Ren, S., Sun, J.: Spatial pyramid pooling in deep convolutional networks for visual recognition. In Fleet, D., Pajdla, T., Schiele, B., Tuytelaars, T., eds.: Computer Vision – ECCV 2014, Cham, Springer International Publishing (2014) 346–361
36. Singh, S., Gupta, A., Efros, A.A.: Unsupervised discovery of mid-level discriminative patches. In Fitzgibbon, A., Lazebnik, S., Perona, P., Sato, Y., Schmid, C., eds.: Computer Vision – ECCV 2012, Berlin, Heidelberg, Springer Berlin Heidelberg (2012) 73–86
37. Donahue, J., Jia, Y., Vinyals, O., Hoffman, J., Zhang, N., Tzeng, E., Darrell, T.: Decaf: A deep convolutional activation feature for generic visual recognition. In Xing, E.P., Jébara, T., eds.: Proceedings of the 31st International Conference on Machine Learning. Volume 32 of Proceedings of Machine Learning Research., Beijing, China, PMLR (22–24 Jun 2014) 647–655
38. Sadanand, S., Corso, J.: Action bank: A high-level representation of activity in video. In: Proceedings of IEEE Conference on Computer Vision and Pattern Recognition. (2012)
39. Yu, R., Li, A., Morariu, V.I., Davis, L.S.: Visual relationship detection with internal and external linguistic knowledge distillation. IEEE International Conference on Computer Vision (ICCV) (2017)
40. Yu, R., Chen, X., Morariu, V.I., Davis, L.S.: The role of context selection in object detection. In: British Machine Vision Conference (BMVC). (2016)
41. Li, A., Morariu, V.I., Davis, L.S.: Selective encoding for recognizing unreliably localized faces. In: 2015 IEEE International Conference on Computer Vision, ICCV 2015, Santiago, Chile, December 7-13, 2015. (2015) 3613–3621
42. Zhao, R., Wu, Z., Li, J., Jiang, Y.: Learning semantic feature map for visual content recognition. In: Proceedings of the 2017 ACM on Multimedia Conference, MM 2017, Mountain View, CA, USA, October 23-27, 2017. (2017) 1291–1299
43. Ballan, L., Castaldo, F., Alahi, A., Palmieri, F., Savarese, S.: Knowledge transfer for scene-specific motion prediction. In: European Conference on Computer Vision (ECCV). (2016)
44. Hays, J., Efros, A.A.: Scene completion using millions of photographs. *ACM Trans. Graph.* **26**(3) (July 2007)
45. Liu, C., Yuen, J., Torralba, A. In: Nonparametric Scene Parsing via Label Transfer. Springer International Publishing, Cham (2016) 207–236
46. Tighe, J., Lazebnik, S.: Superparsing: Scalable nonparametric image parsing with superpixels. In Daniilidis, K., Maragos, P., Paragios, N., eds.: Computer Vision – ECCV 2010, Berlin, Heidelberg, Springer Berlin Heidelberg (2010) 352–365

47. Ballan, L., Bertini, M., Serra, G., Del Bimbo, A.: A data-driven approach for tag refinement and localization in web videos. *Computer Vision and Image Understanding* **140** (Nov. 2015) 58–67
48. Xu, X., Hospedales, T.M., Gong, S.: Discovery of shared semantic spaces for multiscene video query and summarization. *IEEE Transactions on Circuits and Systems for Video Technology* **27**(6) (2017) 1353–1367
49. Yuen, J., Torralba, A.: A data-driven approach for event prediction. In Daniilidis, K., Maragos, P., Paragios, N., eds.: *Computer Vision – ECCV 2010*, Berlin, Heidelberg, Springer Berlin Heidelberg (2010) 707–720
50. Kitani, K.M., Ziebart, B.D., Bagnell, J.A., Hebert, M.: Activity forecasting. In: *Proceedings of the 12th European Conference on Computer Vision - Volume Part IV. ECCV'12*, Berlin, Heidelberg, Springer-Verlag (2012) 201–214
51. Kingma, D.P., Ba, J.: Adam: A method for stochastic optimization. In: *International Conference on Learning Representations (ICLR)*. (2015)